Baltic Astronomy, vol. 13, 555–572, 2004.

SEVEN-COLOR PHOTOMETRY OF THE OPEN CLUSTER NGC 2395 AREA

J. Zdanavičius[1], K. Zdanavičius[1], V. Straižys[1], A. Kazlauskas[1], K. Černis[1], C. W. Chen[2], W. P. Chen[2], R. P. Boyle[3] and G. Tautvaišienė[1]

[1] *Institute of Theoretical Physics and Astronomy, Vilnius University, Goštauto 12, Vilnius, LT 01108, Lithuania*

[2] *Graduate Institute of Astronomy, National Central University, Chung-Li, Taiwan*

[3] *Vatican Observatory Research Group, Steward Observatory, Tucson, Arizona 85721, U.S.A.*

Received 2004 April 15

Abstract. The area of the open cluster NGC 2395 in Gemini is investigated by CCD photometry in the Vilnius seven-color system. Magnitudes, color indices, photometric spectral types, color excesses, interstellar extinctions and distances are determined for 163 stars down to $V = 15.75$ mag in the $25'$ diameter area. Twenty stars at a mean distance of 410 pc are suspected to be cluster members. The main sequence starts at the spectral class F5. Two evolved F5 stars and two red giants are present; the cluster's age should be about 1.5 Gyr. The suspected cluster stars show a differential interstellar extinction ranging from 0.0 to 0.6 mag. Interstellar extinction in the area starts at about the cluster's distance. At larger distances the observed extinction values are scattered between zero and 0.7 mag. Among the suspected cluster members only two K dwarfs are present. It is possible that NGC 2395 has suffered significantly from Galactic tidal distortion on its low-mass star content.

Key words: stars: fundamental parameters – clusters: individual (NGC 2395) – methods: photometric – Vilnius photometric system

1. INTRODUCTION

NGC 2395 is a loose group of stars fainter than 10 mag near the Gemini and Canis Minor border with center equatorial coordinates

$\alpha(2000) = 7^{\rm h}27.1^{\rm m}$ and $\delta(2000) = +13°35'$ and Galactic coordinates ℓ=204.6°, b=+14.0°. The first photographic studies of the cluster by Trumpler (1930) and Collinder (1931) were of low accuracy without good photometric standards. A photographic investigation of the cluster with photoelectric standards in the *UBV* system was published by Chincarini (1963). His *V*, *B*–*V* diagram for 53 stars down to 15 mag did not show any sequences, with *B*–*V* of the stars scattered between 0.3 and 1.4, so the arguments for reality of the cluster were weak. From nine stars, supposed to be main-sequence B stars, Chincarini estimated approximate values of color excess and distance modulus of the cluster: E_{B-V}= 0.72 and $(V - M_V)_0 = 10.4$, corresponding to a distance of 1.2 kpc. These parameters of NGC 2395 for a long time were in use in catalogs of open clusters (e.g., Hagen 1970; Becker & Fenkart 1971; Lynga 1987; Battinelli & Capuzzo-Dolcetta 1991).

However, subsequent investigations of the cluster gave a much smaller color excess and a much closer distance. Dutra & Bica (2000) derive color excesses from the dust emission at 100 μm observed by IRAS and COBE/DIRBE satellite data. Their value for NGC 2395 is $E_{B-V} = 0.10$ only. From the *Hipparcos* parallaxes of eight cluster members Loktin & Beshenov (2001) obtain a distance of 604 pc. The newest version of the WEBDA open cluster data catalog gives E_{B-V} = 0.12 and r = 512 pc (Mermilliod 2004). The same data are given in the catalog of open clusters of Dias et al. (2002).

Trying to test the reality of the cluster and to determine its interstellar reddening we undertook CCD investigation of the cluster area in the *Vilnius* seven-color photometric system.

2. OBSERVATIONS AND REDUCTIONS

The cluster area was observed with the Maksutov 35/51 cm telescope of the Molėtai Observatory equipped with a VersArray 1300B CCD camera of Princeton Instruments. The imaging array of the CCD chip has 1340×1300 pixels of 20×20 μm size. The linear area of the chip is 26.8×26.0 mm, and this corresponds to a field of view 1.26×1.22 degrees. However, in the present paper we present the results of photometry only for the area with a diameter of 25′ centered on the cluster. The chip is cooled by liquid nitrogen to −110°C. A set of round filters of the *Vilnius* system of 6 cm diameter was used. The *U* and *P* filters are made from glasses, and *X*, *Y*, *Z*, *V* and *S*

are interference filters. Details about the instrumentation are given by Zdanavičius & Zdanavičius (2003).

Observations took place on two nights – 2003 March 2/3 (U, Z, V and S filters) and March 6/7 (P, X and Y filters). The exposure time for the U filter was 15 min, for P and X – 10 min, for the remaining filters – from 1 to 3 min. In each filter 2–4 exposures were obtained. The relative air masses ranged between 1.4 and 1.9.

The magnitudes of stars were obtained by aperture photometry using the standard IRAF program package. Registered CCD counts were corrected for a small nonlinearity (Zdanavičius & Zdanavičius 2003). For flat-fielding we used skyflats in each filter, averaging from more than 20 frames taken in evening and/or morning twilight.

The transformation coefficients of magnitudes and color indices to the standard *Vilnius* system were taken from Zdanavičius & Zdanavičius (2003) where they were determined using photoelectric standards in the M67 cluster. Zero points of color equations were based on 12 brightest stars in the area measured photoelectrically (Table 1). Color equations were also verified by synthetic color indices of the *Vilnius* system, calculated for the mean spectral energy distribution curves of stars of different spectral and luminosity classes from Straižys & Sviderskienė (1972). Response curves of the *Vilnius* standard system were taken from Straižys (1992) and of the CCD instrumental system from Zdanavičius & Zdanavičius (2003). The transformation equations determined by the two methods are similar.

At the beginning the instrumental magnitudes m(instr) were determined for individual frames in each filter, then they were averaged. The instrumental color indices m–V(instr) were calculated as differences of the corresponding instrumental magnitudes. After applying color equations the average values of magnitudes V and color indices m–V for each star were obtained.

The V magnitudes and six color indices for 12 standard stars are given in Table 1. The results of CCD photometry for 163 stars down to 15.75 mag are given in Table 2. For the faintest and reddest stars the ultraviolet color indices are of low accuracy and are not given. Color indices with standard errors 0.05–0.10 mag are marked by a colon. The numbers of stars given in Tables 1 and 2 are identified in Figure 1. Optical and physical binary stars were excluded from the catalog.

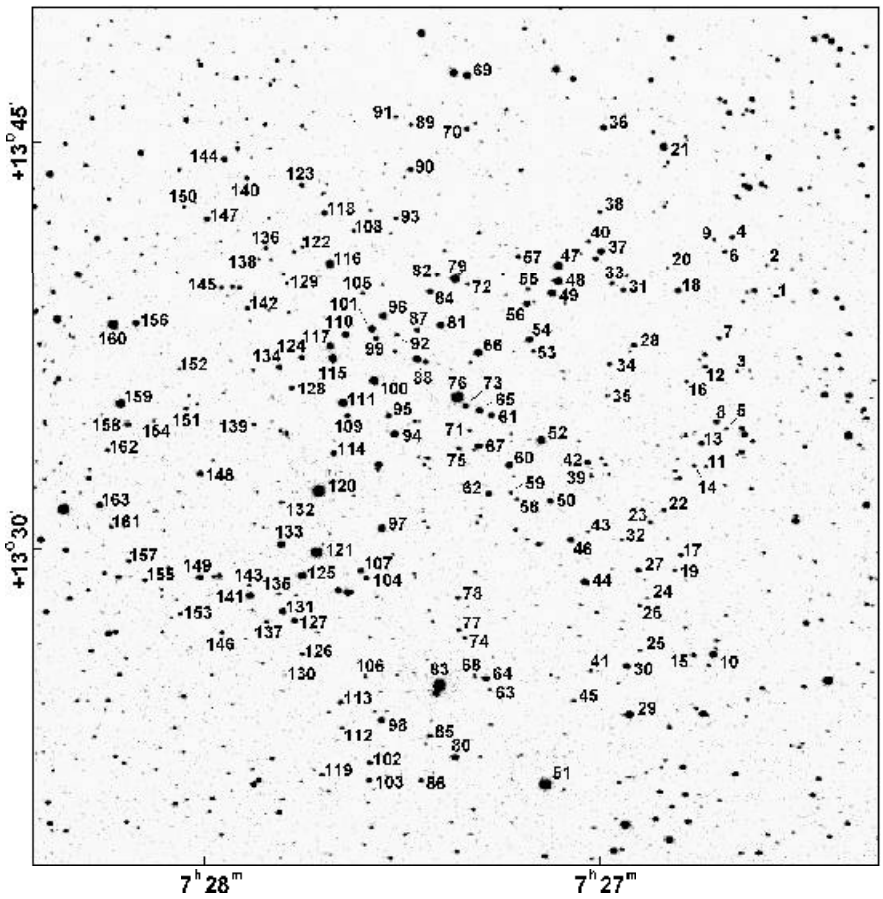

Fig. 1. Identification chart of the NGC 2395 area.

3. CLASSIFICATION, COLOR EXCESSES AND DISTANCES

The stars of Table 2 were classified in MK spectral types using the photometric classification method based on a comparison of 14 reddening-free Q-parameters of the program stars with about 8000 stars with known spectral classification. The method is described in more detail in our earlier papers (see, e.g., Laugalys & Straižys 2002; Straižys et al. 2002). The accuracy of the method for normal solar composition stars is ±1 spectral subclass. The accuracy of luminosity classes is dependent on spectral class: for B, A, F and early G subclasses the accuracy is about ±1 luminosity class but for late G and K–M stars the accuracy is at least twice higher.

Table 1. Photoelectric standards in NGC 2395 measured in 2003 with the 1.5 meter telescope of the Steward Observatory on Mt. Lemmon, Arizona. For each star the second row gives the rms errors.

ID	α (2000)	δ (2000)	V	$U-V$	$P-V$	$X-V$	$Y-V$	$Z-V$	$V-S$	n
47.	07 26 51.2	+13 40 50	11.947	2.288	1.775	1.157	0.479	0.180	0.469	
			0.017	0.015	0.014	0.013	0.014	0.010	0.006	2
49.	07 26 52.2	+13 39 45	12.169	2.179	1.668	1.063	0.443	0.156	0.451	
			0.016	0.015	0.015	0.018	0.017	0.007	0.012	2
52.	07 26 53.9	+13 34 21	11.841	2.266	1.791	1.229	0.505	0.191	0.515	
			0.017	0.016	0.014	0.013	0.006	0.007	0.017	3
76.	07 27 06.8	+13 35 54	9.963	4.912	4.142	2.855	1.050	0.464	0.985	
			0.016	0.016	0.013	0.013	0.005	0.006	0.009	3
88.	07 27 13.0	+13 37 20	12.369	3.656	3.045	2.076	0.804	0.311	0.768	
			0.015	0.017	0.014	0.013	0.004	0.005	0.007	2
97.	07 27 18.6	+13 31 05	11.992	2.290	1.816	1.246	0.520	0.204	0.517	
			0.019	0.017	0.014	0.014	0.008	0.008	0.014	4
100.	07 27 19.6	+13 36 33	11.534	3.577	2.987	2.056	0.776	0.315	0.782	
			0.018	0.016	0.022	0.014	0.016	0.020	0.007	2
111.	07 27 24.4	+13 35 43	11.942	3.637	3.048	2.072	0.784	0.324	0.765	
			0.015	0.016	0.013	0.013	0.006	0.006	0.007	2
115.	07 27 25.9	+13 37 23	11.381	2.341	1.668	0.807	0.308	0.111	0.268	
			0.015	0.015	0.013	0.014	0.004	0.006	0.008	3
116.	07 27 26.2	+13 40 57	11.724	2.434	1.749	0.954	0.379	0.141	0.354	
			0.016	0.015	0.014	0.012	0.005	0.006	0.012	3
120.	07 27 28.2	+13 32 31	10.049	3.496	2.890	1.988	0.788	0.301	0.753	
			0.028	0.020	0.017	0.014	0.006	0.005	0.008	2
121.	07 27 28.6	+13 30 13	10.317	2.243	1.688	1.082	0.467	0.168	0.464	
			0.017	0.016	0.014	0.014	0.004	0.005	0.008	3

The results of the photometric classification of stars are given in the last column of Table 2. The lower-case letters are used to indicate that our spectral types are determined from photometry using the calibration in MK spectral types. For some stars the selected comparison stars were of different luminosity classes. In these cases only the spectral class is given. For a part of stars fainter than 15th mag the classification accuracy was too low, and in such cases we give only an approximate spectral class.

The color excesses E_{Y-V} of the stars were calculated as the differences between the observed $Y-V$ and the intrinsic color indices $(Y-V)_0$ for various spectral and luminosity classes, taken from Straižys (1992, Tables 66–69 and 73). The distance of a star was calculated by the equation:

$$5 \log r = V - M_V + 5 - A_V, \qquad (1)$$

Table 2. The results of CCD photometry of the NGC 2395 field. Identification numbers correspond to the chart given in Figure 1.

ID	α(2000)	δ(2000)	V	$U-V$	$P-V$	$X-V$	$Y-V$	$Z-V$	$V-S$	Ph. sp
1.	7 26 17.6	+13 39 34	15.025	2.394:	1.821	1.304	0.550	0.270:	0.474:	f-g
2.	7 26 19.0	+13 40 46	15.628		1.609:	1.174	0.516	0.110:	0.480:	
3.	7 26 23.7	+13 36 46	15.463	2.046:	2.113:	1.464	0.628	0.225	0.663	g0 V:
4.	7 26 24.4	+13 41 50	14.964	1.145:	2.215:	1.523	0.635	0.202	0.529:	
5.	7 26 25.4	+13 34 39	15.724:		1.887:	1.415:	0.555:	0.304:	0.647:	g
6.	7 26 25.5	+13 41 17	15.061		2.457:	1.751	0.729	0.259	0.698	MDGE-g2
7.	7 26 26.3	+13 38 03	14.904	2.386:	1.852:	1.311	0.567	0.221	0.523	f8 V
8.	7 26 27.0	+13 34 53	13.921	2.485	1.916	1.359	0.579	0.223	0.530	f8 V
9.	7 26 27.1	+13 41 46	15.538		2.061:	1.374	0.572	0.111	0.692	f
10.	7 26 27.6	+13 26 17	12.011	2.776	2.345	1.591	0.611	0.265	0.634	g8 V
11.	7 26 28.7	+13 33 19	15.613:		2.383:	1.625:	0.641:	0.289:	0.666:	g9 V
12.	7 26 28.7	+13 36 59	15.056		1.998:	1.414	0.615	0.253	0.590	sdg3
13.	7 26 29.3	+13 34 11	13.823	2.700:	2.202	1.528	0.597	0.243	0.621	g5 IV
14.	7 26 30.4	+13 33 22	15.186	2.395	1.779	1.223	0.514	0.193	0.481	f5 IV:
15.	7 26 30.8	+13 26 16	14.360		3.543	2.734	1.034	0.457	0.991	k2.5 III
16.	7 26 31.6	+13 36 25	15.475			1.988	0.707	0.407:	0.766	k3 V
17.	7 26 32.7	+13 30 00	14.805	2.314:	1.733	1.213	0.504	0.205	0.511	f-g
18.	7 26 32.7	+13 39 50	13.538	3.114:	2.671	1.866	0.773	0.302	0.748	g8 IV-V
19.	7 26 33.6	+13 29 29	15.665		2.387:	1.616	0.621	0.205	0.662	g
20.	7 26 34.3	+13 40 43	15.758		2.431:	1.720	0.641	0.226	0.688	g5 III:
21.	7 26 34.7	+13 45 14	11.981	2.447	1.903	1.331	0.547	0.205	0.540	f8 V
22.	7 26 35.2	+13 31 41	14.884		3.022:	2.084	0.809	0.328	0.822	k0 IV
23.	7 26 37.3	+13 31 14	14.618			2.631	0.998	0.436	0.914	k2 III
24.	7 26 37.8	+13 28 26	15.664		1.958:	1.345	0.548	0.167	0.584	MDGE-g5
25.	7 26 38.9	+13 26 29	14.736	2.759:	2.390	1.659	0.668	0.284	0.662	g8 V
26.	7 26 39.0	+13 28 07	15.617			1.267:	0.480	0.256	0.576:	g
27.	7 26 39.2	+13 29 29	13.985	2.556:	1.906	1.316	0.553	0.201	0.523	f-g
28.	7 26 39.6	+13 37 47	14.382	2.480:	1.994	1.391	0.593	0.224	0.573	f9 V
29.	7 26 40.7	+13 24 05	12.432	3.674	3.082	2.144	0.843	0.342	0.804	g9 IV:
30.	7 26 41.0	+13 25 54	13.380	2.622	2.173	1.483	0.583	0.247	0.592	g5 V
31.	7 26 41.1	+13 39 53	14.157		3.322:	2.209	0.857	0.370	0.868	k0.5 IV
32.	7 26 41.6	+13 30 37	15.661		1.915:	1.428:	0.587:	0.337:	0.470:	g-k
33.	7 26 42.9	+13 40 07	14.588	2.216:	1.811	1.163	0.508	0.173	0.458	f5 V
34.	7 26 43.3	+13 37 06	14.280	2.483:	1.874	1.285	0.563	0.193	0.568	f-g
35.	7 26 43.8	+13 35 53	15.662		1.805:	1.227	0.525	0.160	0.477:	f-g
36.	7 26 44.0	+13 45 58	13.291	2.303	1.795	1.244	0.522	0.194	0.500	f8 V
37.	7 26 44.5	+13 41 19	12.959	2.369	1.900	1.350	0.553	0.221	0.568	g0 V
38.	7 26 44.7	+13 42 49	15.017		1.795:	1.257	0.532	0.177	0.438	f5 V:
39.	7 26 46.3	+13 32 59	14.595	2.746:	2.109	1.519	0.616	0.233	0.679	g0 III
40.	7 26 46.3	+13 41 44	15.142		1.734	1.248	0.557	0.206	0.521	f-g
41.	7 26 46.6	+13 25 44	14.828	2.592:	1.952	1.316	0.554	0.227	0.566	MDGE-g5
42.	7 26 46.7	+13 33 30	13.498	3.080	2.602	1.733	0.654	0.296	0.660	k0 IV-V
43.	7 26 46.8	+13 30 55	15.665			1.739	0.710	0.411	0.635	g6 III
44.	7 26 47.4	+13 29 01	12.410	2.195	1.661	1.140	0.466	0.182	0.456	MDG-g
45.	7 26 49.3	+13 24 36	15.268		1.763:	1.211	0.484	0.113	0.522	f7 V
46.	7 26 49.5	+13 30 37	13.919	2.476	1.913	1.386	0.598	0.213	0.562	MDGE-g5
47.	7 26 51.1	+13 40 50	11.948	2.289	1.742	1.170	0.476	0.174	0.472	f8 IV-V
48.	7 26 51.2	+13 40 13	12.226	2.419	1.930	1.361	0.550	0.220	0.562	g1 V
49.	7 26 52.1	+13 39 45	12.137	2.210	1.662	1.099	0.464	0.172	0.450	f5 IV-V
50.	7 26 52.6	+13 32 02	13.803	3.608:	3.046	2.083	0.808	0.380	0.775	k1 V
51.	7 26 53.7	+13 21 30	10.085	2.214	1.688	1.145	0.466	0.176	0.470	f5 V
52.	7 26 53.9	+13 34 21	11.836	2.275	1.781	1.240	0.505	0.189	0.505	f9 V
53.	7 26 55.1	+13 37 36	15.336		2.109	1.505	0.656	0.185	0.599	f7 V
54.	7 26 55.6	+13 38 01	12.634	3.160	2.569	1.827	0.749	0.291	0.723	g2 III
55.	7 26 55.8	+13 39 55	14.861			2.155	0.822	0.380	0.760	k1 IV
56.	7 26 56.0	+13 39 22	13.118	3.509:	2.863	1.998	0.807	0.316	0.767	g8 III-IV
57.	7 26 57.2	+13 41 10	14.572		2.134	1.478	0.600	0.208	0.588	g0 III-IV
58.	7 26 57.7	+13 32 08	15.659		1.912:	1.422	0.559	0.197	0.630	g1 V
59.	7 26 58.7	+13 32 24	15.563		1.826:	1.316	0.571	0.154	0.579	f-g
60.	7 26 58.9	+13 33 26	12.777	3.328	2.788	1.931	0.775	0.323	0.745	g9 IV

Table 2 (continued)

ID	α (2000)	δ (2000)	V	$U-V$	$P-V$	$X-V$	$Y-V$	$Z-V$	$V-S$	Ph. sp
61.	7 27 01.5	+13 35 14	13.675	2.450:	1.712	1.037	0.406	0.140	0.393	f2 III
62.	7 27 02.1	+13 32 22	13.805		3.173	2.152	0.835	0.310	0.833	g9 III
63.	7 27 02.1	+13 25 03	15.739		2.121:	1.455	0.619	0.168	0.634	f8 V:
64.	7 27 02.7	+13 25 28	12.434	2.070	1.569	1.058	0.443	0.161	0.439	f5 V
65.	7 27 03.5	+13 35 25	13.188	2.548	2.061	1.444	0.570	0.215	0.585	g2 IV-V
66.	7 27 03.6	+13 37 33	12.388	2.355	1.881	1.310	0.537	0.208	0.542	f9 V
67.	7 27 03.6	+13 34 08	12.223	2.358	1.828	1.256	0.526	0.189	0.515	f7 V
68.	7 27 04.4	+13 25 32	15.072	2.337:	2.092	1.510	0.631	0.181	0.689	
69.	7 27 04.9	+13 47 57	12.375	3.567	2.929	2.056	0.821	0.320	0.790	g6/7 III
70.	7 27 04.9	+13 45 57	14.191	2.592	2.117	1.478	0.624	0.209	0.619	g2 V
71.	7 27 04.9	+13 34 39	15.565		2.449:	1.623	0.597	0.167	0.712	g
72.	7 27 05.1	+13 40 08	15.607		1.943:	1.367	0.592	0.223:	0.554	f8-g1
73.	7 27 05.5	+13 35 35	14.022	2.575	2.113	1.486	0.617	0.274	0.605	g2 V:
74.	7 27 05.9	+13 26 59	15.288		1.998:	1.383	0.589	0.231:	0.551	f-g
75.	7 27 06.7	+13 34 02	14.972	2.336:	1.843	1.339	0.587	0.252	0.503	f8 V
76.	7 27 06.8	+13 35 55	9.967	4.933	4.156	2.860	1.056	0.467	1.000	k3 III
77.	7 27 06.9	+13 27 16	14.972	2.236:	1.706	1.124	0.491	0.155	0.477	f5 V
78.	7 27 07.0	+13 28 30	14.374	2.422:	1.759	1.173	0.491	0.190	0.475	f
79.	7 27 07.0	+13 40 20	11.719	4.377	3.734	2.566	0.974	0.414	0.930	k1.5 III
80.	7 27 07.6	+13 22 30	12.949	2.314	1.818	1.283	0.520	0.213	0.532	f8 V
81.	7 27 09.2	+13 38 35	12.818	4.019	3.373	2.333	0.895	0.356	0.859	k0 III
82.	7 27 09.8	+13 40 29	14.252	2.610:	2.027	1.426	0.603	0.203	0.619	f-g
83.	7 27 10.3	+13 25 17	9.685	3.020	2.575	1.732	0.644	0.308	0.671	k1 V
84.	7 27 10.9	+13 39 52	13.652	3.728:	2.996	2.129	0.837	0.321	0.781	g2 Ib
85.	7 27 11.4	+13 23 19	14.512		2.451	1.755	0.709	0.298	0.715	g8 V
86.	7 27 12.8	+13 21 39	14.367	2.622:	1.797	1.133	0.495	0.176	0.475	f
87.	7 27 12.9	+13 38 25	13.998	2.304	1.801	1.241	0.547	0.215	0.460	f6 V
88.	7 27 12.9	+13 37 20	12.362	3.650:	3.053	2.072	0.809	0.310	0.775	g8 III
89.	7 27 13.6	+13 46 07	15.096		2.019	1.421	0.601	0.278	0.538	g1.5 V:
90.	7 27 13.7	+13 44 27	13.470	2.892	2.335	1.612	0.667	0.264	0.658	g2 IV-V
91.	7 27 15.9	+13 46 25	14.819		3.179:	2.139	0.832	0.335	0.788	k0 III
92.	7 27 16.0	+13 38 15	14.983	2.213:	1.690	1.166	0.500	0.133	0.493	f5 V
93.	7 27 16.0	+13 42 37	15.079		1.996	1.411	0.600	0.234	0.605	g1 V
94.	7 27 16.4	+13 34 35	13.429	3.591:	2.897	2.269	1.002	0.438	1.066	g
95.	7 27 17.3	+13 35 15	14.070	2.294	1.747	1.195	0.519	0.169	0.526	f5 V
96.	7 27 18.1	+13 38 59	12.299	3.034	2.538	1.759	0.733	0.277	0.670	g5 IV
97.	7 27 18.5	+13 31 06	11.980	2.268	1.795	1.250	0.512	0.197	0.509	f9 V
98.	7 27 18.8	+13 23 57	13.325	2.370	1.899	1.338	0.544	0.221	0.547	g0 V
99.	7 27 19.3	+13 38 08	14.078	2.299	1.661	1.065	0.440	0.145	0.450	f2 III
100.	7 27 19.5	+13 36 33	11.528	3.596	2.986	2.053	0.805	0.326	0.789	g8 IV
101.	7 27 19.9	+13 38 28	12.764	2.631	2.086	1.478	0.622	0.223	0.610	g0 V
102.	7 27 20.6	+13 22 21	14.552	2.700:	2.093	1.435	0.600	0.225	0.625	g0 V
103.	7 27 20.8	+13 21 42	14.187	2.453	1.982	1.400	0.600	0.210	0.582	g0 V
104.	7 27 21.0	+13 29 13	14.379	2.309	1.781	1.248	0.532	0.193	0.530	f8 V
105.	7 27 21.2	+13 39 48	14.718	2.447:	2.016	1.465	0.596	0.159	0.616	
106.	7 27 21.3	+13 25 34	14.677	2.323:	1.875	1.277	0.554	0.189	0.553	f9 V
107.	7 27 21.8	+13 29 31	13.220	2.337	1.776	1.262	0.547	0.210	0.531	f8 V
108.	7 27 22.6	+13 42 11	15.214		1.702	1.128	0.478	0.154	0.467	f5 V
109.	7 27 23.7	+13 35 17	14.484	2.459	2.153	1.485	0.608	0.200	0.622	g2 V:
110.	7 27 24.0	+13 38 16	12.945	2.538	2.094	1.462	0.597	0.233	0.594	g2 V
111.	7 27 24.4	+13 35 43	11.946	3.677	3.065	2.072	0.792	0.332	0.765	k0 III-IV
112.	7 27 24.9	+13 23 40	15.644		2.380:	1.628:	0.639	0.184	0.717	
113.	7 27 25.1	+13 24 36	13.855	2.303:	1.847	1.367	0.594	0.205	0.572	f-g
114.	7 27 25.8	+13 33 54	13.296	3.291	2.803	1.898	0.682	0.343	0.761	k2 V
115.	7 27 25.9	+13 37 23	11.390	2.316	1.607	0.807	0.306	0.115	0.268	a8 IV:
116.	7 27 26.2	+13 40 57	11.724	2.422	1.692	0.961	0.379	0.140	0.346	f2 III
117.	7 27 26.3	+13 37 50	12.254	4.454:	3.818	2.544	0.950	0.418	0.893	k2 III
118.	7 27 27.0	+13 42 52	14.065	2.373	1.798	1.242	0.532	0.173	0.535	f5 V
119.	7 27 28.0	+13 21 56	14.854		2.895:	2.008	0.719	0.422	0.772	k3 V
120.	7 27 28.2	+13 32 31	10.030	3.461	2.886	1.990	0.783	0.301	0.748	g7 III
121.	7 27 28.6	+13 30 13	10.331	2.213	1.644	1.077	0.453	0.161	0.462	f5 IV

Table 2 (continued)

ID	α(2000)	δ(2000)	V	$U-V$	$P-V$	$X-V$	$Y-V$	$Z-V$	$V-S$	Ph. sp
122.	7 27 30.4	+13 41 34	15.596		2.397:	1.679	0.663	0.260	0.514	g
123.	7 27 30.5	+13 43 56	14.349		3.593:	2.502	0.870	0.579	1.056	k7-m0 V
124.	7 27 30.8	+13 37 26	13.990	3.194:	2.492	1.741	0.731	0.290	0.703	g
125.	7 27 30.9	+13 29 21	11.959	2.217	1.740	1.188	0.482	0.181	0.495	f8 V
126.	7 27 31.0	+13 26 24	15.129		2.629:	1.748	0.688	0.315	0.680	g8 V
127.	7 27 32.1	+13 27 41	13.529	2.563	2.021	1.396	0.599	0.235	0.560	f8 IV
128.	7 27 32.2	+13 36 19	14.331	2.762:	2.088	1.471	0.615	0.246	0.618	f9
129.	7 27 32.9	+13 40 13	15.109			2.303	0.764	0.487	0.870	k4.5 V
130.	7 27 33.6	+13 25 36	15.743		1.701	1.198	0.508	0.161	0.526	MDGE-g5
131.	7 27 33.9	+13 28 01	12.999	3.829:	3.310	2.220	0.840	0.353	0.833	k1 III
132.	7 27 34.0	+13 32 05	14.917	2.326:	1.720	1.178	0.510	0.121	0.569	f-g
133.	7 27 34.1	+13 30 32	12.740	3.675:	3.033	2.086	0.858	0.332	0.782	g8 III
134.	7 27 34.1	+13 37 04	12.846	4.242:	3.630	2.509	0.956	0.394	0.916	k1 III
135.	7 27 34.5	+13 28 42	15.737		1.862:	1.289	0.554	0.124:	0.621:	f-g
136.	7 27 36.0	+13 41 32	15.041		2.071:	1.968	0.736	0.385	0.743	k
137.	7 27 36.4	+13 27 39	15.219		2.154:	1.508	0.631	0.140	0.605:	f
138.	7 27 37.1	+13 41 09	15.749			1.906:	0.725:	0.348:	0.706:	k1 V
139.	7 27 38.1	+13 34 56	14.774	2.438:	1.905	1.323	0.560	0.181	0.630	f8 V
140.	7 27 38.9	+13 44 10	14.805		2.043	1.371	0.573	0.174	0.604	f-g
141.	7 27 39.0	+13 28 39	12.416	2.573	2.045	1.406	0.567	0.220	0.565	f9 IV-V
142.	7 27 39.0	+13 39 17	14.578		3.137:	2.158	0.864	0.349	0.773	g8 III-IV
143.	7 27 39.1	+13 29 00	15.523		2.205:	1.547	0.636	0.201	0.677	g
144.	7 27 42.4	+13 44 53	13.778	3.512:	2.742	1.938	0.792	0.274	0.776	MDGE-g8
145.	7 27 42.9	+13 40 06	15.197		2.870:	1.967	0.723	0.353	0.773	k2 V
146.	7 27 43.3	+13 27 14	15.078		2.274	1.680	0.653	0.289	0.712	g
147.	7 27 44.9	+13 42 38	13.650	2.305	1.840	1.263	0.555	0.178	0.542	f7 V
148.	7 27 46.4	+13 33 10	13.303	2.300	1.766	1.181	0.501	0.183	0.485	f5 V
149.	7 27 46.6	+13 29 19	13.027	2.966	2.440	1.648	0.649	0.288	0.652	g8 V
150.	7 27 48.5	+13 43 06	15.475		1.776	1.131	0.490	0.204	0.449:	f5 IV-V
151.	7 27 48.5	+13 35 33	14.684	2.520:	1.811	1.251	0.529	0.192	0.577	MDGE-g8
152.	7 27 49.7	+13 37 02	15.234	2.319:	1.841	1.350	0.564	0.174	0.537	f-g
153.	7 27 49.7	+13 27 57	15.344		2.261:	1.590	0.665	0.304	0.683	g5 V
154.	7 27 53.6	+13 35 08	15.572		2.135:	1.514	0.642	0.246	0.621:	g0 V
155.	7 27 55.1	+13 29 12	14.710	2.628:	2.093	1.417	0.587	0.243	0.621	g0 V
156.	7 27 56.2	+13 38 46	13.214	2.241	1.765	1.260	0.543	0.194	0.540	g0 V md
157.	7 27 57.5	+13 29 55	15.076		2.079:	1.438	0.625	0.254	0.495:	g0 V
158.	7 27 57.6	+13 34 59	13.003	4.154:	3.481	2.374	0.925	0.374	0.886	k1 III
159.	7 27 58.7	+13 35 45	11.559	2.093	1.423	0.655	0.258	0.085	0.203	b8/a7
160.	7 27 59.6	+13 38 42	11.096	2.330	1.823	1.243	0.519	0.189	0.503	f8 V
161.	7 28 00.1	+13 31 12	14.879		2.679	1.771	0.685	0.304	0.638	k0 IV
162.	7 28 00.6	+13 34 03	14.988	2.623:	1.835	1.286	0.531	0.201	0.509	g0 V
163.	7 28 02.0	+13 32 01	13.069	4.207:	3.645	2.456	0.920	0.416	0.869	k1 IV

where $A_V = 4.16E_{Y-V}$. The absolute magnitudes were taken from the Straižys (1992) tabulation according to the spectral and luminosity classes, with a correction of -0.1 mag, bringing the M_V scale to the new distance modulus of the Hyades ($V-M_V = 3.3$, Perryman et al. 1998). For the majority of stars the absolute magnitude error is <0.5 mag.

The V magnitudes, $Y-V$ color indices and photometric spectral types of the stars are repeated in Table 3. The table also contains absolute magnitudes M_V, extinctions A_V and distances r. The values of distances at $r > 200$ pc are rounded to the nearest number multiple of 10.

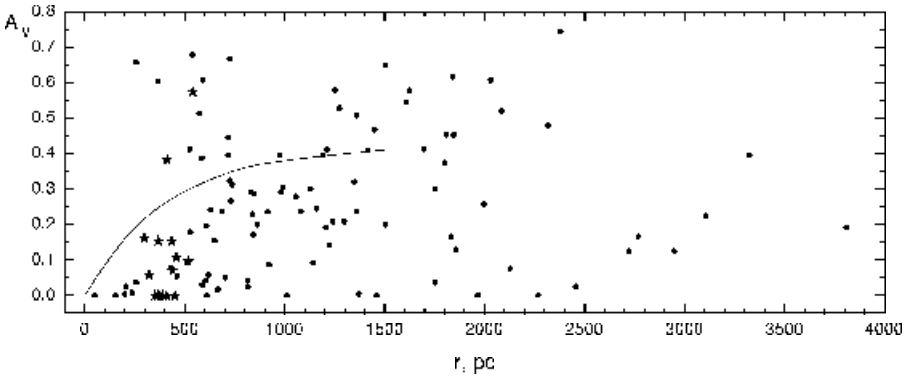

Fig. 2. Interstellar extinction vs. distance in the NGC 2395 area. The exponential Parenago curve for $A_0 = 1.05$ mag/kpc and $\beta = 0.095$ kpc is shown. These coefficients in the Parenago formula are taken from Sharov (1963) for the Galactic coordinates of the cluster. The suspected members of the cluster are shown by $\star$ symbols.

4. INTERSTELLAR EXTINCTION VS. DISTANCE

Figure 2 shows the interstellar extinction A_V plotted against distance r in parsecs. The following conclusions can be made.

1. The stars with zero extinction are distributed up to 2 kpc distances. Probably, they are seen through transparent windows in the Galactic dust layer.

2. The rise of interstellar extinction takes place at 400 pc. Approximately at this distance a dust cloud or a group of clouds should be present. These clouds give the maximum extinction 0.7 mag. At a distance of 400 pc and a Galactic latitude of 14° the clouds should be about 100 pc above the Galactic plane.

3. The most distant stars of solar chemical composition in the area are: No. 20 ($V = 15.76$, g5 III, 9.4 kpc), No. 43 ($V = 15.67$, g6 III, 8.3 kpc), No. 91 ($V = 14.82$, k0 III, 5.9 kpc), No. 23 ($V = 14.62$, k2 III, 4.9 kpc) and No. 15 ($V = 14.36$, k2.5 III, 4.4 kpc). Eight stars in the area (Nos. 6, 24, 41, 44, 46, 130, 144 and 151) were classified as metal-deficient giants of spectral class G (see Table 2). Some of them are fainter than 14th mag, thus they may be among the most distant stars in our sample, but their accurate absolute magnitudes and distances are not known.

4. The exponential Parenago formula with coefficients $A_0 = 1.05$ mag/kpc and $\beta = 0.095$ kpc (Parenago 1945; Sharov 1963) for this

Table 3. Photometric classification, extinctions and distances.

ID	Ph.sp.	V	M_V	Y–V	A_V	r (pc)
3.	g0 V	15.463	4.3	0.628	0.41	1420
7.	f8 V	14.904	4.0	0.567	0.24	1360
8.	f8 V	13.921	4.0	0.579	0.29	840
10.	g8 V	12.011	5.5	0.611	0.00	200
11.	g9 V	15.613	5.7	0.641	0.09	920
13.	g5 IV	13.823	3.0	0.597	0.00	1460
14.	f5 IV:	15.186	2.5	0.514	0.22	3110
15.	k2.5 III	14.360	0.5	1.034	0.62	4360
16.	k3 V	15.475	6.6	0.707	0.03	590
18.	g8 IV-V	13.538	4.3	0.773	0.57	540
20.	g5 III:	15.758	0.9	0.641	0.00	9370
21.	f8 V	11.981	4.0	0.547	0.15	370
22.	k0 IV	14.884	3.1	0.809	0.45	1850
23.	k2 III	14.618	0.6	0.998	0.57	4880
25.	g8 V	14.736	5.5	0.668	0.24	630
28.	f9 V	14.382	4.1	0.593	0.30	990
29.	g9 IV	12.432	3.1	0.843	0.68	540
30.	g5 V	13.380	5.0	0.583	0.05	460
31.	k0.5 IV	14.157	3.1	0.857	0.53	1280
33.	f5 V	14.588	3.5	0.508	0.20	1510
36.	f8 V	13.291	4.0	0.522	0.05	700
37.	g0 V	12.959	4.3	0.553	0.10	520
38.	f5 V:	15.017	3.5	0.532	0.30	1750
39.	g0 III	14.595	1.5	0.616	0.19	3810
42.	k0 V	13.498	5.9	0.654	0.06	320
43.	g6 III	15.665	0.9	0.710	0.17	8310
45.	f7 V	15.268	3.8	0.484	0.00	1970
47.	f5 V	11.948	3.5	0.476	0.08	470
48.	g1 V	12.226	4.4	0.550	0.00	370
49.	f5 IV-V	12.137	3.0	0.464	0.02	670
50.	k1 V	13.803	6.1	0.808	0.66	260
51.	f5 V (IV:)	10.085	(2.5)	0.466	0.02	(330)
52.	f9 V	11.836	4.1	0.505	0.00	350
53.	f7 V	15.336	3.8	0.656	0.65	1500
54.	g2 III	12.634	1.0	0.749	0.58	1630
55.	k1 IV	14.861	3.1	0.822	0.26	2000
56.	g8 III-IV	13.118	2.0	0.807	0.51	1360
58.	g1 V	15.659	4.4	0.559	0.04	1760
60.	g9 IV	12.777	3.1	0.775	0.40	720
61.	f2 III	13.675	1.7	0.406	0.02	2460
62.	g9 III	13.805	0.8	0.835	0.40	3330
63.	f8 V:	15.739	4.0	0.619	0.45	1810
64.	f5 V	12.434	3.5	0.443	0.00	610
65.	g2 IV -V	13.188	3.8	0.570	0.04	820
66.	f9 V	12.388	4.1	0.537	0.07	440
67.	f7 V	12.223	3.8	0.526	0.11	460

Table 3. (continued)

ID	Ph.sp.	V	M_V	Y–V	A_V	r (pc)
69.	g7 III	12.375	0.8	0.821	0.54	1610
70.	g2 V	14.191	4.6	0.624	0.27	730
73.	g2 V:	14.022	4.6	0.617	0.24	690
75.	f8 V	14.972	4.0	0.587	0.32	1350
76.	k3 III	9.967	0.7	1.056	0.61	540
77.	f5 V	14.972	3.5	0.491	0.13	1860
79.	k1.5 III	11.719	0.6	0.974	0.58	1250
80.	f8 V	12.949	4.0	0.520	0.04	600
81.	k0 III	12.818	0.7	0.895	0.52	2090
83.	k1 V	9.685	6.1	0.644	0.00	52
85.	g8 V	14.512	5.5	0.709	0.41	520
87.	f6 V	13.998	3.6	0.547	0.28	1060
88.	g8 III	12.362	0.8	0.809	0.41	1700
89.	g1.5 V:	15.096	4.5	0.601	0.19	1200
90.	g2 IV-V	13.470	3.8	0.667	0.44	720
91.	k0 III	14.819	0.7	0.832	0.26	5920
92.	f5 V	14.983	3.5	0.500	0.17	1830
93.	g1 V	15.079	4.4	0.600	0.21	1240
95.	f5 V	14.070	3.5	0.519	0.24	1160
96.	g5 IV	12.299	3.0	0.733	0.51	570
97.	f9 V	11.980	4.1	0.512	0.00	380
98.	g0 V	13.325	4.3	0.544	0.06	620
99.	f2 III	14.078	1.7	0.440	0.17	2770
100.	g8 IV	11.528	3.1	0.805	0.60	370
101.	g0 V	12.764	4.3	0.622	0.38	410
102.	g0 V	14.552	4.3	0.600	0.29	980
103.	g0 V	14.187	4.3	0.600	0.29	830
104.	f8 V	14.379	4.0	0.532	0.09	1140
106.	f9 V	14.677	4.1	0.554	0.14	1220
107.	f8 V	13.220	4.0	0.547	0.15	650
108.	f5 V	15.214	3.5	0.478	0.08	2130
109.	g2 V:	14.484	4.6	0.608	0.20	860
110.	g2 V	12.945	4.6	0.597	0.15	440
111.	k0 III-IV	11.946	1.9	0.792	0.24	920
114.	k2 V	13.296	6.4	0.682	0.01	240
115.	a8 IV:	11.390	1.8	0.306	0.02	820
116.	f2 III	11.724	1.7	0.379	0.00	1010
117.	k2 III	12.254	0.6	0.950	0.37	1800
118.	f5 V	14.065	3.5	0.532	0.30	1130
119.	k3 V	14.854	6.6	0.719	0.08	430
120.	g8 III	10.030	1.7	0.783	0.30	400
121.	f5 IV	10.331	(2.5)	0.453	0.00	(370)
123.	k7 V-m0 V	14.349	8.4	0.870	0.00	155
125.	f8 V	11.959	4.0	0.482	0.00	390
126.	g8 V	15.129	5.5	0.688	0.32	730
127.	f8 IV	13.529	2.7	0.599	0.41	1210
129.	k4.5 V	15.109	7.0	0.764	0.00	410

Table 3. (continued)

ID	Ph.sp.	V	M_V	Y–V	A_V	r (pc)
131.	k1 III	12.999	0.7	0.840	0.12	2720
133.	g8 III	12.740	0.8	0.858	0.62	1840
134.	k1 III	12.846	0.7	0.956	0.61	2030
138.	k1 V	15.749	6.1	0.725	0.31	740
139.	f8 V	14.774	4.0	0.560	0.21	1300
141.	f9 IV -V	12.416	3.4	0.567	0.20	610
142.	g8 III-IV	14.578	2.0	0.864	0.74	2380
145.	k2 V	15.197	6.4	0.723	0.18	530
147.	f7 V	13.650	3.8	0.555	0.23	840
148.	f5 V	13.303	3.5	0.501	0.17	840
149.	g8 V	13.027	5.5	0.649	0.16	300
150.	f5 IV-V	15.475	3.0	0.490	0.12	2950
153.	g5 V	15.344	5.0	0.665	0.40	980
154.	g0 V	15.572	4.3	0.642	0.47	1450
155.	g0 V	14.710	4.3	0.587	0.24	1080
157.	g0 V	15.076	4.3	0.625	0.40	1190
158.	k1 III	13.003	0.7	0.925	0.48	2320
160.	f7 V	11.096	3.9	0.519	0.08	260
161.	k0 IV	14.879	3.1	0.685	0.00	2270
162.	g0 V	14.988	4.3	0.531	0.00	1370
163.	k1 IV	13.069	3.1	0.920	0.67	730

Table 4. Suspected members of NGC2395.

ID	Ph. sp.	V	A_V	r (pc)	ID	Ph. sp.	V	A_V	r (pc)
18.	g8 IV-V	13.54	0.57	540	76.	k3 III	9.97	0.61	540
21.	f8 V	11.98	0.15	370	97.	f9 V	11.98	0.00	380
37.	g0 V	12.96	0.10	520	101.	g0 V	12.76	0.38	410
42.	k0 V	13.50	0.06	320	110.	g2 V	12.94	0.15	440
47.	f5 V	11.95	0.08	470	120.	g8 III	10.03	0.30	400
48.	g1 V	12.23	0.00	370	121.	f5 IV	10.33	0.00	(370)
51.	f5 (IV)	10.08	0.00	(330)	125.	f8 V	11.96	0.00	390
52.	f9 V	11.84	0.00	350	129.	k4.5 V	15.11	0.00	410
66.	f9 V	12.39	0.07	440	149.	g8 V	13.03	0.16	300
67.	f7 V	12.22	0.11	460	160.	f7 V	11.10	0.08	260

sky position gives the maximum extinction of ∼0.4 mag. For $A_0 =$ 1.5 mag/kpc and the same β the maximum extinction is ∼0.7 mag. These values are consistent with the observed distribution of stars.

5. The IRAS and COBE/DIRBE 100 μm dust emission map of the area (see Schlegel et al. 1998 and http://skyview.gsfc.nasa.gov) shows somewhat uneven distribution of dust emission in our area: the strongest emission is seen in its south-western part. However,

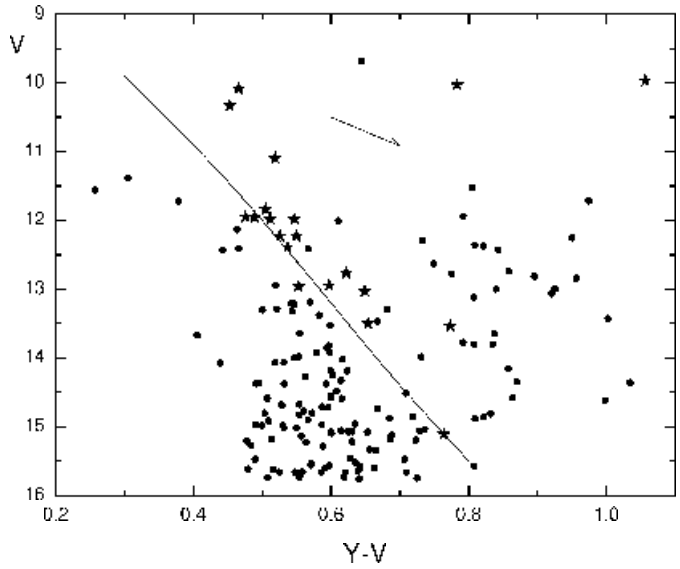

Fig. 3. Color-magnitude diagram in the NGC 2395 area. The symbols ⋆ mark 20 suspected members of the cluster. The Hyades main sequence shifted to the unreddened cluster stars is shown. The arrow marks the shift of a star with the interstellar reddening $E_{Y-V} = 0.10$ mag.

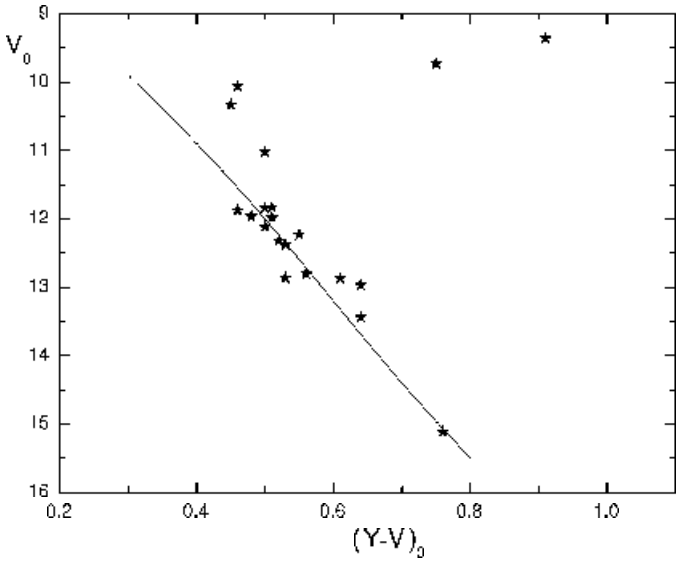

Fig. 4. Intrinsic color-magnitude diagram for the suspected cluster members.

our results fail to show any extinction differences in the area on macro scale. The main source of the observed extinction differences in Figure 2 probably is related with the random distribution of small dust clouds. As a result, in some directions we observe the transparent windows and in other directions – overlappings of several small clouds.

5. ON THE CLUSTER MEMBERS

For the estimation of the membership of the cluster and for the determination of its physical properties we have plotted the color-magnitude diagram for the area stars (Figure 3). Already Chincarini (1963) has shown that in the V, B–V diagram the main sequence of the cluster is not well defined. Figure 3 confirms this conclusion. This may mean that either the cluster is unreal or the scarce stars of the cluster cannot be distinguished among the field stars.

Trying to identify possible cluster members we have selected 20 stars which according to their distances and spectral types might belong to a physical group. These stars are listed in Table 4 and shown in Figures 2 and 3 by 'star' symbols. Their distances are between 260 pc and 540 pc; the average distance is 410 pc. This scatter may be explained by the distance determination errors which are estimated to be $\sigma{\sim}20\%$. Different values of A_V (from 0.0 to 0.6 mag) of these stars might be explained by the spatial proximity of the cluster to the dust cloud and its clumpiness. Therefore in Figure 3 some of these stars are displaced right and down from their intrinsic positions due to reddening and extinction. This prevents seeing typical cluster sequences in the color-magnitude diagram.

Figure 4 shows the intrinsic positions of these 20 stars. In the sky they are scattered in an oblong area of $12' \times 23'$ with the long axis approximately parallel to the Galactic equator. At a distance of 410 pc this corresponds to 1.4×2.7 pc. In the same volume of space in the solar neighborhood only four stars (the Sun and the α Centauri triple system) are present. This is a serious argument for confirmation of the cluster reality.

Our attempts to find reliable proper motions in the NGC 2395 area have failed. Proper motions are available for most of the area stars in the USNO-B Catalog (Monet et al. 2003). However, at the accuracy of the available proper motions, the suspected cluster stars do not show any peculiar motion with respect to the surrounding field stars.

The stars in Table 4 include all nine stars used by Chincarini

(1963) to estimate color excess and distance of the cluster. Chincarini has accepted (without arguments) that these stars belong to B-type main sequence, while in reality they are F and G main-sequence stars. Therefore, the parameters of the cluster determined by Chincarini were false.

If these 20 stars form a real cluster, it is possible to estimate its age. The hottest main-sequence stars are of spectral class F5. In this respect NGC 2395 is similar to the well-known cluster NGC 752 with the hottest stars of spectral classes F1–F2 and the 1.3–1.6 Gyr age (Bartašiūtė et al. 2004). Both clusters are almost at the same distance from the Sun: 440 pc and 410 pc for NGC 752 and NGC 2395, respectively.

HR diagrams of both clusters are also similar. Both show the evolutionary deviation from the main sequence of a similar size. But the difference is in the number of stars in the deviated main sequence: in NGC 752 there are more than twenty of such stars, while in NGC 2395 we have found only the two suspects: No. 51 and No. 121. In Table 2 we give their spectral classes f5 V and f5 IV which follow from their comparison stars. If the luminosity class of star 51 is really V, it may be a field star. These two stars were not considered taking the distance average of the suspected cluster members (410 pc).

Among the possible members of NGC 2395 there are two red giants, Nos. 120 (g8 III) and 76 (k3 III). These two stars are at the center of the observed clustering. Their spectral classes and absolute magnitudes given in Table 3 were determined by another, more accurate, method using the calibrated interstellar reddening-free Q_{UPY}, Q_{XZS} and Q_{XZS}, Q_{XYZ} diagrams. The data for the two stars given in Table 4 correspond to these spectral types and absolute magnitudes. Their calculated distances within errors coincide with the cluster distance estimated from the main-sequence stars. Star No. 120 probably is on the red clump corresponding to central helium burning, while star No. 76 is on the red giant branch.

6. MORPHOLOGY OF THE CLUSTER

The distribution of member stars within a cluster should change during its evolution. The structure of the parent molecular cloud, from which the star cluster is formed, plays an important role on the initial stellar distribution. Mutual gravitational interaction then modifies the distribution of member stars. As the cluster ages, external disturbances such as the Galactic tidal force or encounters with

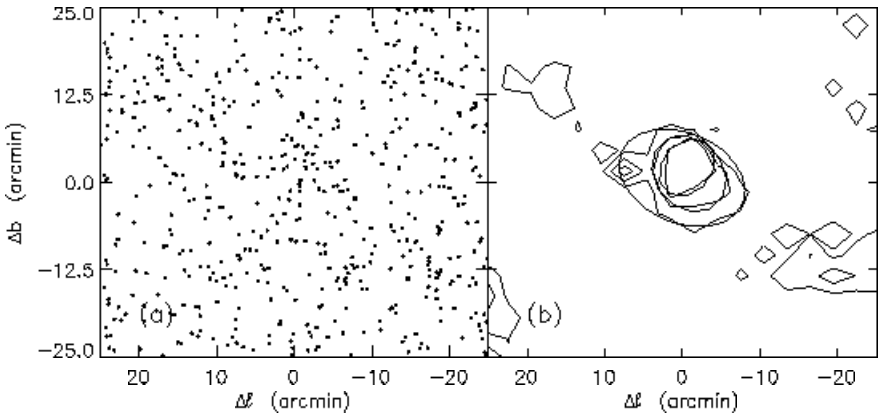

Fig. 5. Panel (a): 2MASS field for morphology determination of NGC 2395; panel (b): contour plot of NGC 2395, see the text for more explanations.

giant molecular clouds would eventually disintegrate the cluster (see e.g. Bergond et al. 2001).

Chen et al. (2004) have studied the morphology of Galactic open clusters with the help of the 2MASS (Two-Micron All-Sky Survey) point-source catalog. They concluded that almost all open clusters are elongated. This phenomenon is evident even among the youngest clusters of a few million years age. As these clusters would have no sufficient time to fully relax dynamically, their morphology must bear a direct imprint of the structure of the parent molecular clouds. Furthermore, the cluster ellipticity is found to correlate with the age and the height above the Galactic plane, suggesting the influence of the Galactic tidal force.

NGC 2395 may be an old open cluster whose dynamical evolution has been affected by the Galactic perturbation forces. We analyzed the morphology of NGC 2395 with the 2MASS point-source catalog in the K_s band. The Palomar DSS images show clearly dozens of bright stars distributed sparsely in an elongated way. The 2MASS data also show a concentration of relatively bright stars. The stars fainter than $K_s \sim 13$ mag display no obvious density enhancement against field stars. It is likely that low-mass member stars have been "evaporated" over the age of NGC 2395.

We applied to NGC 2395 the same star-counting technique as described in Chen et al. (2004). Figure 5 shows the distribution of stars of NGC 2395. It is seen that the star group is elongated, with an outer boundary of an eccentricity ∼0.7 and a core of an

eccentricity ∼0.6. The cluster is located in the thick disk, about 100 pc above the Galactic plane. Probably it has suffered a significant tidal distortion on its shape and has lost most of its former members.

6. CONCLUSIONS

1. Interstellar extinction versus distance diagram shows the presence of a group of dust clouds at a distance of ∼400 pc. The maximum extinction given by the clouds is 0.7 mag.

2. Sixteen stars of spectral types F5 V – K4 V, two evolved stars on the deviated main sequence and two red giants may belong to a physical group at the distances between 260 pc and 540 pc, the average value is 410 pc. This range of distances may be explained by the errors of absolute magnitudes. Color excesses of these stars may be different due to clumpiness of the dust cloud. The cluster is at 100 pc above the Galactic plane.

3. The metallicity of the suspected cluster stars should be close to solar as all comparison stars, which are most similar photometrically to the cluster stars, have normal chemical composition.

4. The deviated main sequence at F5 spectral class shows that the cluster age should be close to 1.5 Gyr. In this respect NGC 2395 is very similar to NGC 752.

5. According to probabilistic star-counting analysis, NGC 2395 may have suffered significantly from the Galactic tidal distortion on its shape and population.

6. For a better understanding of the cluster, careful determination of proper motions and radial velocities of stars would be helpful.

ACKNOWLEDGMENTS. This work was supported by the National Science Council of Taiwan, the Ministry of Education and Science of Lithuania, and by the American Astronomical Society Chretien Grant of 2000. We are grateful to V. Laugalys for his help in the data processing and for useful comments.

REFERENCES

Bartašiūtė S., Deveikis V., Straižys V. 2004, Baltic Astronomy (submitted)

Battinelli P., Capuzzo-Dolcetta R. 1991, MNRAS, 249, 76

Becker W., Fenkart R. 1971, A&AS, 4, 241

Bergond G., Leon S., Guibert J. 2001, A&A, 377, 462

Chen W., Chen C. W., Shu C. G. 2004, AJ, in press

Chincarini G. 1963, Mem. Soc. Astron. Italiana, 34, 23

Collinder P. 1931, Annals Leiden Obs., 2

Dias W. S., Alessi B. S., Moitinho A., Lepine J. R. D. 2002, A&A, 389, 871

Dutra C. M., Bica E. 2000, A&A, 359, 347

Hagen G. L. 1970, *An Atlas of Open Cluster Colour-Magnitude Diagrams*, Publ. D. Dunlap Obs., Toronto, vol. 4

Laugalys V., Straižys V. 2002, Baltic Astronomy, 11, 205

Loktin A. V., Beshenov G. V. 2001, Astr. Letters, Moscow, 27, 386

Lynga G. 1987, Open Cluster Data, 5th Edition, Lund Observatory, CDS VII-92A

Mermilliod J.-C. 2004, A Site Devoted to Stellar Clusters WEBDA, http://obswww.unige.ch/webda

Monet D. G., Levine S. E., Canzian B. et al. 2003, AJ, 125, 984

Parenago P. P. 1945, AZh, 22, 129

Perryman M. A. C., Brown A. G. A., Lebreton Y. et al. 1998, A&A, 331, 81

Schlegel D. J., Finkbeiner D. P., Davis M. 1998, ApJ, 500, 525

Sharov A. S. 1963, AZh, 40, 900 = Soviet Astron., 7, No. 5

Straižys V. 1992, *Multicolor Stellar Photometry*, Pachart Publishing House, Tucson, Arizona

Straižys V., Černis K., Kazlauskas A., Laugalys V. 2002, Baltic Astronomy, 11, 231

Straižys V., Sviderskienė Z. 1972, Bull. Vilnius Obs., No. 35, 3

Trumpler R. J. 1930, Bull. Lowell Obs., 14, 171

Zdanavičius J., Zdanavičius K. 2003, Baltic Astronomy, 12, 642